Enabling Bayesian Inference for the Astronomy Masses

Performance Report submitted by M. D. Weinberg, PI
Period: 3/15/08–3/14/09
Grant Number: NNG-06-GF25G

1 Executive summary

Active development proceeded in all of the research topics. Major accomplishments include:

1. Development of statistical methodology
    - Improved and tested our tempered simulation. Based on discussions with Michael Lavine, we implemented a generalized concept of "hot" chains beyond powering-up the posterior distribution.
    - Continued development of our hybrid multiple-level MCMC methodology, benchmarking the strategy for an upcoming methods paper
    - Investigated effect of indistinguishability in mixture components on convergence and bias in posterior distributions
2. Development of persistence technology
    - Completed, debugged and tested serialization and persistence for nearly all BIE methods.
3. Preparation for final code release
    - Continuing to "plug holes" in documentation
    - Improved reliability of autoconf-based configuration, adding automatic warnings about dependencies
    - Code sanitized for adherence to ANSI C++ standards, latest versions of the Boost and GTK libraries
4. Astronomical applications

- Designed tests using a suite of synthetic galaxy images to benchmark our new GALFIT-like galaxy image analyzer which we have code-named GALPHAT for GALaxy PHotometric ATtributes. We have begun analyzing 2MASS galaxy images and have begun a collaboration with the COSMOS group and have tested GALPHAT on their images.
- Using our hybrid simulated tempering–differential evolution MCMC algorithm, we have achieved convergent posterior distributions for our semi-analytic-model (BIE–SAM) code. We are continuing to augment the problem definition to include more complex "real-world" data sets such as Tully-Fisher and HI mass distributions.
- We have completed and tested our color-magnitude diagram *generator* based on the most recent isochrone tracks that included the AGB and post-AGB stellar evolution phases. We are beginning our test its performance on simulated and 2MASS We may now make start count predictions along any line of sight given a star-formation history, metallicity distribution in space. We will test both our model and methodology using 2MASS LMC/SMC data.

2 No-cost extension

Although our award date is March 15, 2006, for some reason, we were not notified until June 2006. We were not able to get a post-doc on-board until the following year, so we requested an institutional 12 month extension. If possible, I would like to request an additional six month extension beyond this point to give the post-doc a full 3 years and to give us time to finish up the final publications and code release.

3 Research milestones and summary

I will detail some of the advances below and end with a list of Milestones for the final period.

1 System development

The implementation of the persistence subsystem is now complete, documented, and extensively tested. We are currently using it in-house for all of our projects and it will be in the final code release.

We have used the persistence subsystem to implement a full checkpointing scheme. Checkpointing goes beyond save/restore in that it saves what is happening in the *middle* of a Markov chain. Running these chains is the most time-consuming part of running the BIE, and thus the most vulnerable to crashes, etc. Checkpointing allows one to resume after a crash, or if one needed or desired to abandon a computation for some reason. We can trigger checkpointing based on the number of iterations since the last checkpoint, the amount of time that has passed, or upon user request via typing a certain control character on the console.

In addition, the user may use checkpoint save sets to recall the state of previous simulation for future updates based on new data or for model comparison and selection. For now, storage of save-sets is the user's responsibility. However, this implementation lays the groundwork for a future SVN-based data+metadata repository.

Other system developments include generalizing and increasing the interoperability of the class structure to permit unanticipated future uses.

2 GALPHAT

2.1 Motivation

We had originally intended to use BIE as a back end for GALFIT . GALFIT is a modular package written to perform two dimensional image decompositions for galaxies which are from nearby to distant (Peng et al. 2002). We found that the pixel integration and PSF convolution were too inaccurate and time-consuming for our application which necessitated our rewriting the model generation code. We have code-named the new parameter determination package GALPHAT for GALaxy PHotomometric ATtributes. Our combination of this approach with our Bayesian Inference Engine back end, which will allow GALFIT-based investigations of the full posterior not just the extremum mode, and will establish proper prior distributions, which allow inferences using Bayes Factors over a wide variety of competing models and hypotheses.

As a reminder, our likelihood function is

$$P(D \mid \theta) = \frac{\exp(-\frac{1}{2}[\mathbf{D}-\mathbf{M}(\theta)]^t \mathbf{W}[\mathbf{D}-\mathbf{M}(\theta)])}{(2\pi)^{Npix/2} \mid \mathbf{W} \mid^{-1/2}} \tag{1}$$

where $\mathbf{D}$ is data vector($N_x \times N_y$), $\mathbf{M}(\theta)$ is a model vector and $\mathbf{W}$ is a weight matrix for pixel value. Our models include with a mixture of Sérsic profile a user-supplied prior for each parameter. Each Sérsic profile has 8 free parameters in the fit: centroid of the profile(x_c, y_c), integrated magnitude(M_{tot}) which is related with Σ_e, effective radius(r_e), Sérsic index(n), axis ratio(b/a), position angle(PA) and diskiness/boxiness(c). In addition, we specify a model for the sky background with 3 free parameters:sky level, sky gradient in X, Y direction.

During the last 12 months, GALPHAT has been tested using simulated galaxies, incorporating the advanced features of BIE such hierarchical simulation levels, multiple MCMC algorithms and persistence. We performed more comprehensive tests based on ensemble images of single Sérsic galaxies simulated with different galaxy structural parameters (magnitude, size, Sérsic index, axis ratio, position angle). As a function of the signal-to-noise ratio (S/N, using signal and noise within half-light radius). Figures 1 and 2 show the difference between the input parameters and the output parameters derived from the whole ensemble of posterior distributions. Overall, parameter dispersion becomes smaller as S/N increases (see Fig. 1). Surprisingly, the dispersion in structural parameters decreases only slightly with increasing image size (see Fig. 2). The Sérsic index and galaxy half-light radius are biased high due to the nature of Sérsic profile, while magnitude posterior distribution is not skewed. The unchanging 99.7% confidence interval is due to the angular degeneracy for face-on galaxies.

By experimenting with different MCMC algorithms, priors and proposal widths, we identified combinations that yielded a robust posterior for 2MASS bulge-disk decomposition analysis. These include an observationally motivated non-informative prior for galaxy half-light radius and assuming a common center for all profiles in the mixture. For limited number of test cases, More comprehensive tests are ongoing. In addition, we have characterized 2MASS sample properties by deriving

luminosity function with different measuring techniques and comparing with the previously published data (Kochanek et al. 2001). Our results are very similar except for slight difference in normalization, which may be due to differences in sky coverage.

3 SAMS–BIE

Galaxy formation and evolution has been one of the most challenging problems in astrophysics owing to the interplay of multiple physical processes on hugely disparate time and length scales. Modeling or simulating galaxies from the first principle is impossible currently, semi-analytic models (SAMs) use phenomenological prescriptions of the processes too difficult to study from first principles. By comparing the SAM predictions to observations, researchers hope to identify the key processes controlling galaxy formation. SAMs are attractive, and have a remarkable number of citations, for the following reasons. First, they are built upon the CDM structure formation framework, proven to be a successful model on cosmological scales. Second, standard CDM techniques produce a large sample of galaxies using Monte Carlo methods for observational comparisons. Third, and most important for its popularity, SAMs have a much lower computational cost than direct simulation.

Nevertheless, a number of inherent thorny problems in this approach may limit its contribution to true understanding. Typically in semi-analytic modeling, a subset of model parameters are held fixed while others are adjusted to match observations (e.g. the galaxy luminosity function or stellar mass function, the Tully-Fisher relation, and color distribution). If the match is unsatisfactory, the practitioner either further adjusts some of the parameters or changes the model until the "best fit" is achieved. This procedure is flawed for a number of reasons:

1. The goodness of fit is usually assessed "by eye", and the agreement between the model with the observations becomes a subjective proxy for model selection. There is no attempt to account for the prior information or the model dimensionally in rejecting competing hypotheses.

2. Owing to our lack of first-principle knowledge, the recipes live in a high-dimensional parameter space. Since some if not all of the parameters are expected to be covariant, the isosurfaces of the likelihood function are almost certainly complex and multi-modal. Exploring this space "by hand" is impossible. The significance of a "reasonable" agreement found after a small number of attempts is impossible to quantify and the complex likelihood function produces tremendous difficulty in determining how to improve the agreement of the model.

3. Given the topological complexity of likelihood function in the high-dimensional model space, its restricted variation in a small subset of parameters (a "cut") may have little bearing on the true probability over a properly marginalized distribution. In other words, because the influence of any single process is conditional on all the physical processes in the entire galaxy formation model, the knowledge of the variation obtained by adjusting a single parameter is also conditional on the fixed parameters in the model. Insight gained from a particular cut is therefore likely to be circumstantial rather than informative.

Probabilistically, the SAM method is a model selection problem. Bayesian inference provides a consistent approach to all of the problems identified above, automatically providing the entire probability distribution of the parameters. Our goal is put semi-analytic modeling on rigorous probabilistic footing. To incorporate the approach into the framework of Bayesian inference, we have implemented a SAM that incorporates all of mainstream SAMs. This will allow us to compare with published results and test various proposed parameterizations.

3.1 Our SAM

We have implemented recipes for the following processes: 1) radiative cooling; 2) star formation; 3) supernova feedback; 4) galaxy mergers; 5) stellar population synthesis; and 6) dust extinction. A flowchart describing the structure of the model is shown in Figure 3. The parameters are summarized in the Table 1. Our fiducial model is a restriction to 13 free parameters, since the remainder do not influence our prediction of the stellar mass function. For each parameter, we choose a prior distribution that brackets the values that other groups have adopted and as required for physical consistency. Figure 4 outlines the computation, typical of most Bayesian posterior simulations: the MCMC algorithm provides proposal parameter vectors for the SAM, and the SAM predicts the galaxy populations using the parameter set. The likelihood is evaluated by comparing the predictions with the observations, and is returned to the MCMC procedure. The converged posterior samples contain the full probability distribution of the model parameters for the given observational data.

Using the Bayesian approach, we expect to fully investigate the posterior probability distribution of the model for given observations. First, we should be able to layout the degeneracy between parameters if it exist. Second, we can marginalize the parameters that we are not interested in and sketch the probability distribution of the model parameters. Third, we can integral the posterior probability over the entire parameter space to derive the Bayes factor to test one hypothesis against another.

3.2 Example: the stellar mass function

We simplify the problem by assuming the error in each stellar mass bin is independent. A paper in preparation describes the effected of correlated error in detail. With this simplification, the likelihood is written as

$$L(\Phi_{\rm obs}|\theta) = L_0 \exp\left\{ -\sum_i \frac{(\log\Phi_{i,\rm obs} - \log\Phi_{i,\rm mod})^2}{2\sigma^2_{i,\rm obs}} \right\}, \tag{2}$$

where L_0 is an arbitrary normalization factor, $\Phi_{i,\rm obs}$ and $\Phi_{i,\rm mod}$ are the stellar mass functions of the ith bin from observation and the model (resp.) for a given parameter set θ, and $\sigma_{i,\rm obs}$ is the variance of the observed logarithmic stellar mass function. Since the model variance is smaller than the data variance as we tested using different merger tree sets, we ignore the model variance in the likelihood.

We now describe the results of three example inferences. In the first, Model 0, we adopt weakly informative priors for all the 13 parameters; in the second one, Model 1, we adopt narrow priors to some of the parameters; in the third, Model 2, we further restrict the prior distributions to reproduce

Table 1: Model parameters

#	Parameter	Meaning	Prior	Posterior
1	$\log M_{cc}\,(\mathrm{M}_\odot)$	cooling cut-off halo mass	[1.5 , 4.5] [1.5 , 4.5] [1.5 , 4.5]	[2.01, 2.97] [3.27, 4.47] [3.15, 4.47] [1.95, 2.37]
2	$\log \alpha_{SF}$	star formation efficiency power-law amplitude	[-3, 0] [-3, 0] [-3, 0]	[-2.31, -0.150] [-2.25, -1.83] [-1.71, -0.870]
3	β_{SF}	star formation efficiency power-law index	[-1, 12] [-0.2, 0.2] [-0.2, 0.2]	[-0.870, 10.6] [-0.2, 0.2] [-0.2, 0.2]
4	$\log V_{SF}$ (km/s)	star formation law turn-over halo circular velocity	[1.5, 3.0] [2.1, 2.3] [2.1, 2.3]	[1.52, 2.54] [2.1, 2.3] [2.1, 2.3]
5	$\log \Sigma_{SF}\,(\mathrm{M}_\odot/\mathrm{pc}^2)$	star formation threshold gas surface density	[-2, 2] [0.8, 1.2] [0.8, 1.2]	[-1.88, 1.96] [0.8, 1.2] [0.8, 1.2]
6	$\log \alpha_{SN}$	SN feedback energy fraction	[-3, 1] [-3, 1] [-3, 1]	[-2.96, -0.720] [-0.400, 0.960] [0.160, 0.960] [-1.04, -0.320]
7	$\log \alpha_{RH}$	SN feedback reheating power-law amplitude	[-4, 2] [-4, 2] [-4, 2]	[-3.94, 1.34] [-2.02, -0.820] [0.260, 1.22] [1.70, 1.94]
8	β_{RH}	SN feedback reheating power-law index	[0, 12] [0, 12] [-0.2, 0.2]	[0.360, 11.6] [6.60, 10.4] [-0.2, 0.2]
9	$\log e_W$	fraction of SN feedback energy used for powering wind	[-3, 0] [-3, 0] [-3, 0]	[-2.97, -0.210] [-2.97, -1.35] [-0.270, -0.0300]
10	$\log f_{RI}$	fraction of re-infall ejected hot gas	[-3, 0] [-3, 0] [-3, 0]	[-2.97, -0.0300] [-2.97, -0.0300] [-2.97, -0.630]
11	$\log f_{DF}$	merging time-scale in dynamical friction time-scale	[-2, 2] [-2, 2] [-2, 2]	[0.520, 1.96] [0.840, 1.96] [-1.96, -0.520]
12	$\log \alpha_{SB}$	merger triggered star burst efficiency power-law amplitude	[-3, 0] [-3, 0] [-3, 0]	[-2.97, -0.0300] [-2.97, -0.0900] [-2.97, -0.150]
13	β_{SB}	merger triggered star burst efficiency power-law index	[0, 2] [0, 2] [0, 2]	[0.0200, 1.94] [0.020, 1.98] [0.020, 1.98]
14	α_{EJ} (fixed)	SN feedback cold gas ejection power-law amplitude	0.0	0.0
15	β_{EJ} (fixed)	SN feedback cold gas ejection power-law index	0.0	0.0
16	f_{MG} (fixed)	major merger minor merger threshold	0.3	0.3

the Croton model (Croton et al. 2006). We choose narrow priors for parameters that do not affect the predictions. These include the power-law dependence of the star formation efficiency on the halo circular velocity. For these cases, we set the prior to be consistent with the existing models (Croton model, in particular).

The marginalized posterior distribution of key parameters for each of the models is shown in Figure 5, 6, and 7 (respectively). Clearly, some are only weakly constrained. For example, $e_{\rm W}$, the efficiency of SN feedback for powering galactic wind, is weakly constrained by the stellar mass function. In addition to that, we see some parameters are strongly correlated. For example, the β_{SF}—β_{RH}, α_{RH}—β_{RH}, and M_{cc}—f_{DF} dimensions. These correlations are understandable in the context of CDM based galaxy formation models. To suppress the star formation in small halos, either the star formation rate must be intrinsically small or the SN feedback must be enhanced to keep these systems from active star formation. The posterior distribution of β_{SF}—β_{RH} implies either a sharply declining star formation efficiency against small halo mass or a steep SN feedback reheating halo mass dependence. The distribution of α_{RH}—β_{RH}, the two parameters in the power-law formalism for the SN feedback reheating model, are strongly correlated. Finally, the correlation $M_{\rm cc}$ and $f_{\rm DF}$ implies that sufficient numbers of massive galaxies require either rapid merging with little hot-gas cooling or slow merging but rapid hot-gas cooling.

On the other hand, some parameters are tightly constrained by the stellar mass function. Figure 5 reveals a sharp turn-over halo circular velocity ($\approx$ 160km/s) in the star-formation efficiency law. In other words, the star formation efficiency must decrease sharply with decreasing halo mass. The parameters, β_{SF} and β_{RH}, are also tightly constrained. We find higher values for these parameters (6 for β_{SF} and 8 for β_{RH}) than found in early SAM results.

In Model 1, we choose a narrow prior $[-0.2, 0.2]$ for $\beta_{\rm SF}$ consistent with published SAM investigations (e.g. Croton et al. 2006 use 0 for this parameter). Based on Model 0, we apply narrow Gaussian priors for $\log V_{\rm SF} \sim N(2.2, 0.02)$, based on observational evidence of a star-formation threshold at approximately $10\,{\rm M}_{\odot}/{\rm pc}^2$ we choose $\log \Sigma_{\rm SF} \sim N(1.0, 0.03)$. Figure 6 shows the posterior distribution. We note the following differences. First, a quick comparison with Figure 5 shows the effect of the narrow priors improves the constraints in other dimensions. For example, we have constrained the star formation law to have shallow dependence on halo mass dependence. Therefore, the SN feedback reheating is forced to be a steep function

Previous studies have concluded that the SAMs over predict the number of small galaxies when star-formation efficiency is a shallow function of halo mass, but the fit remains "reasonable." Is a "reasonable" fit maintained in a high-dimensional parameter space keeping the star formation and SN feedback power-laws flat? To address this, we further add a narrow prior for the parameter $\beta_{RH} \in [-0.2, 0.2]$. Figure 7, shows the results. The mode moves dramatically with respect to Model 1. To compensate for the weaker SN reheating in small halos due to the flat SN feedback reheating law, the model increases the reheating and wind (the mode in $\log \alpha_{\rm RH} - \log \varepsilon_{\rm W}$ plane moves from the lower-left corner to the upper-right corner). The shape of the correlation between $\log \alpha_{\rm SN}$ and $\log \alpha_{\rm RH}$ obtained in this inference is similar to the results of Henriques et al. (2008) using Croton model ($\alpha_{\rm SN}$ and $\alpha_{\rm RH}$ in our model are equivalent to $\varepsilon_{\rm halo}$ and $\varepsilon_{\rm disk}$ in Croton model).

From these simple examples, we conclude that a pinning a parameter without prior information leads to a spurious inference. Since many of the parameters are correlated, inappropriately fixing one parameter will unrealistically constrain to other parameters.

4 Star count analyses

With deep data sets of asymptotic giant branch (AGB) stars from nearby galaxies such as the Large and the Small Magellanic Clouds (LMC and SMC, respectively), modeling their structure using theoretical models of stellar evolution has become feasible. The Magellanic Clouds are particularly good candidates for such modeling given their proximity to the Milky Way and given that extinction towards the Clouds is small and their stars are very well resolved.

Color–magnitude diagrams (CMDs) produced from isochrones of stellar evolution models, combined with age–metallicity relations and a model of the galaxies' stellar structures are used as input data (prior) for the Bayesian Inference machinery.

4.1 Generating CMDs from Isochrones

As a first step, the generation of CMDs from sets of theoretical isochrones was solved. This step turned out to be more way more involved than anticipated. Briefly, theoretical isochrones, available at five different metallicities (see Cioni et al. 2006) were used, using a sequence of interpolations (in stellar mass, metallicity, and age). On top of that, star–formation rate (SFR) histories (SFRHs) and age–metallicity relations (AMRs) had to be provided (see Pagel & Tautvaisiene 1998, Carrera et al. 2008). The initial mass function (IMF) is assumed to be independent of age and equal to the log–normal function of Chabrier (2001).

The combination of these ingredients produce CMDs for sets of stars within the desired ranges of age and metallicity. These CMDs then have to be convolved with a model of the structure of the galaxy (incl. a realistic treatment of extinction towards the line–of–sight of the galaxy) to produce full model CMDs that can be compared with observed ones. The existing BIE machinery already included a very simple model for the different ingredient; and the different parts had to be replaced with the more sophisticated new model generator.

4.2 Integration with BIE

After a very stringent set of tests the CMD generator was integrated with the existing Bayesian Inference machinery. Unfortunately, the CMD generator was originally coded in C, whereas BIE uses a very elegant version of C++, which resulted in a whole series of necessary re–writes, bugs (some of which took quite a while to find) and bug fixes.

In addition, several parts of the CMD generator turned out to be too slow and had to be optimized. In the first version of the modeling, a set of stars with fixed SFRHs and AMRs is being used as input data for the BIE, which uses a simple model for the galaxy structure (varying different structure parameters). In the original version of the code, querying the set of stars (which BIE does many times) took over 300 seconds for a sample of about forty thousand stars. This turned running a single step inside BIE into a major endeavor and made running a realistic BIE simulation with thousands of steps prohibitively expensive.

After a very intensive study of data structures, the new version of the code now takes a few seconds for the same operation (very detailed tests of the results ensured that the routine returns the correct data). Furthermore, the code has been expanded to enable reading previously generated data sets from disk, which, for the aforementioned sample of forty thousand stars, eliminates another twelve hundred seconds of time. Ten minutes might not seem all that much, but it becomes very

relevant especially in the debugging and early development phase. The CMD generator is now fully integrated, optimized, and tested to run with BIE.

4 Milestones for the final period

1. Statistical & MCMC development

   - Continued testing and exploration of novel techniques for rapid improvement of mixing and convergence for high-dimensional complex posterior distributions typical of real-world astronomical problems.
   - We will provide qualitative suggestions and wisdom for choosing various MCMC algorithms and diagnostic procedures, a suite of examples, test code, and complete documentation.

2. GALPHAT

   - We will finish the GALPHAT performance tests including budge-disk analysis, using simulated galaxies and finish the GALPHAT methods paper (Yoon et al. 2009)
   - We will implement a Minimum Covariance Determinate Estimator for calculating Bayes factors and characterize the power of BIE in model comparison problem using simulated galaxy images.
   - We will synthetically sample single Sérsic galaxies from a distribution of parameter space (e.g. luminosity function, Sérsic index distribution, galaxy size distribution). From these galaxy samples, we will derive posterior distributions using different priors and compare the result to the input distribution of simulated galaxy population. This will enable us to access the importance of prior for galaxy image analysis and provide guidance to future users.
   - We will complete the analysis of (approx. 500) of 2MASS sample using GALPHAT and derive structural properties, which will be compared to previously published observations including, but not limited to bulge-disk ratio, magnitude-size relation, observed distribution of size and Sérsic index. Informed by these results, we will proceed to analyze the full sample of 2000 2MASS galaxy images.

3. Semi-analytic models

   - The error in stellar mass function includes the counting noise in each stellar mass bin *and* the systematic uncertainties that are correlated across all the bins. In particular, the uncertainties of the stellar population synthetic model, which is used to estimate the stellar mass from the observed stellar light, affects the entire stellar mass function. We will explore the more direct alternative approach: predicting luminosity function directly from the model and use the observed luminosity function.

- We will implement the newest stellar population synthesis model (BC07), which incorporates the thermally pulsing AGB star into the model and work with the K-band luminosity function.
- We will explore the sensitivity to the CB07 and BC03 models and anticipate an analysis using Bayes factor model selction.
- Lu et al. (in prep.) has demonstrated that the model recipes for radiative cooling predict different cooling rate because of their different implementation, and more importantly, none of the existing model predict cooling rate agree with current SPH simulation. The models in general under predict the cold model accretion for small halos and over predict cooling rate in massive halos. Lu et al. has proposed a new model that incorporates cold mode accretion explicitly into SAM. We are planning to implement the new model into the BIE-SAM study. Using observations as stellar mass function HI mass function etc., we can study if the cold model accretion is significantly supported by observation.

4. Star count analyis

- We will test more complex galaxy structure models in addition to the simple exponential disk model used to date.
- A realistic model for extinction towards the SMC/LMC is already included in the module and is thus not required. We will explore generalizations for other nearby galaxies.
- Once all model parts are production ready, with realistic structure models will start to model the structure of the LMC and SMC. We anticipate minor work on optimizing the calculation of the spatial domain, but the other model components are fully optimized and thoroughly tested. Once the mechanism has been successfully applied to either the LMC or SMC, applying it to other galaxies requires no additional work. We anticipate astronomical results and a paper by the end of the extended award period.

Bibliography

Bell, E. F., McIntosh, D. H., Katz, N., & Weinberg, M. D. 2003, ApJS, 149, 289
Braak, C.J.F.T. 2006, Stat. Comput., 16, 239
Carrera R., Gallart C., Hardy E., Aparicio A., Zinn R., 2008, AJ, 135, 836
Chabrier G., 2001, ApJ, 554, 1274
Cioni M.R.L., Girardi L., Marigo P., Habing H.J., 2006, A&A, 448, 77
Croton, D. J., et al. 2006, MNRAS, 365, 11
Henriques, B., Thomas, P., Oliver, S., & Roseboom, I. 2008, arXiv:0810.2548
Kochanek, C. S., et al. 2001, ApJ, 560, 566
Lu, Y., Katz, N., Mo, H., & Weinberg, M. D. 2009, in preparation
Peng, C. Y., Ho, L. C., Impey, C. D., & Rix, H.-W., 2002, AJ, 124, 266
Pagel B.E.J., Tautvaisiene G., 1998, MNRAS, 299, 535
Weinberg, M. D., Moss, E. B. 2009, in preparation
Yoon, I., Weinberg, M. D. & Katz, N. 2009, in preparation

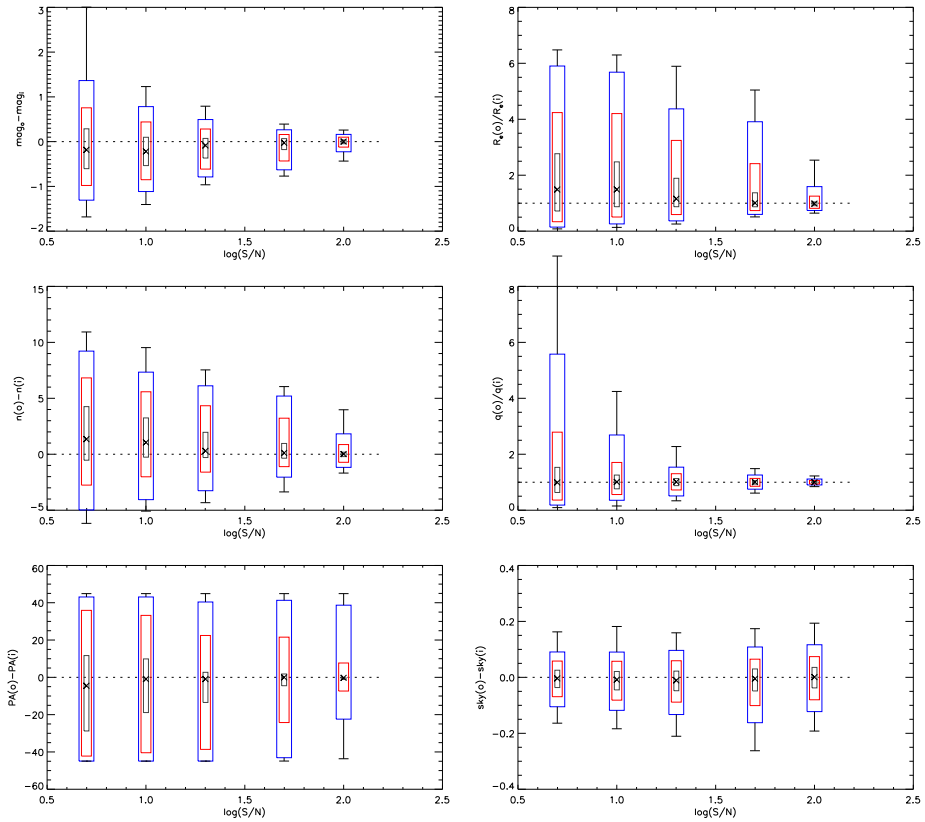

Figure 1: Parameter residual as a function of SN. From left to right and upper to lower, magnitude residual(output-input), half-light radius scaled by input value, Sérsic index residual, axis ratio scaled by input value, position angle residual, sky residual. Every SN bin contains 100 galaxies with different input structural parameters; input half-light radius is uniform in 6-14 pixel, input axis ratio is uniform in 0.1-1.0, input Sérsic index is uniform in 0.7-7.0, position angle is uniform in 0-90. SN bin is 5.0, 10.0, 20.0, 50.0, 100.0 each. charcoal, red, blue boxes include 68.3, 95.4, 99.73% confidence interval corresponding 1,2,3 sigma. And cross is posterior median and two bars at the end is min and max of data. PSF FWHM is 2.96, far larger than the minimum half-light radius of galaxies.

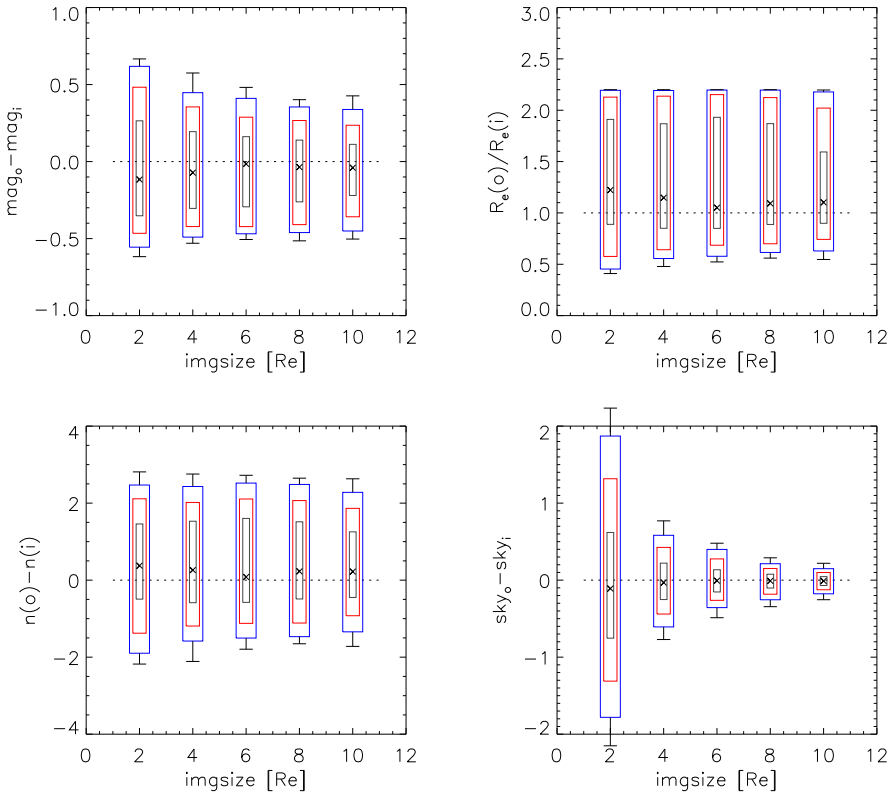

Figure 2: Parameter residual as a function of image size (denoted as a 1/2 of one side of square image) compare to galaxy half-light radius. All symbols are same as in Fig. 1.

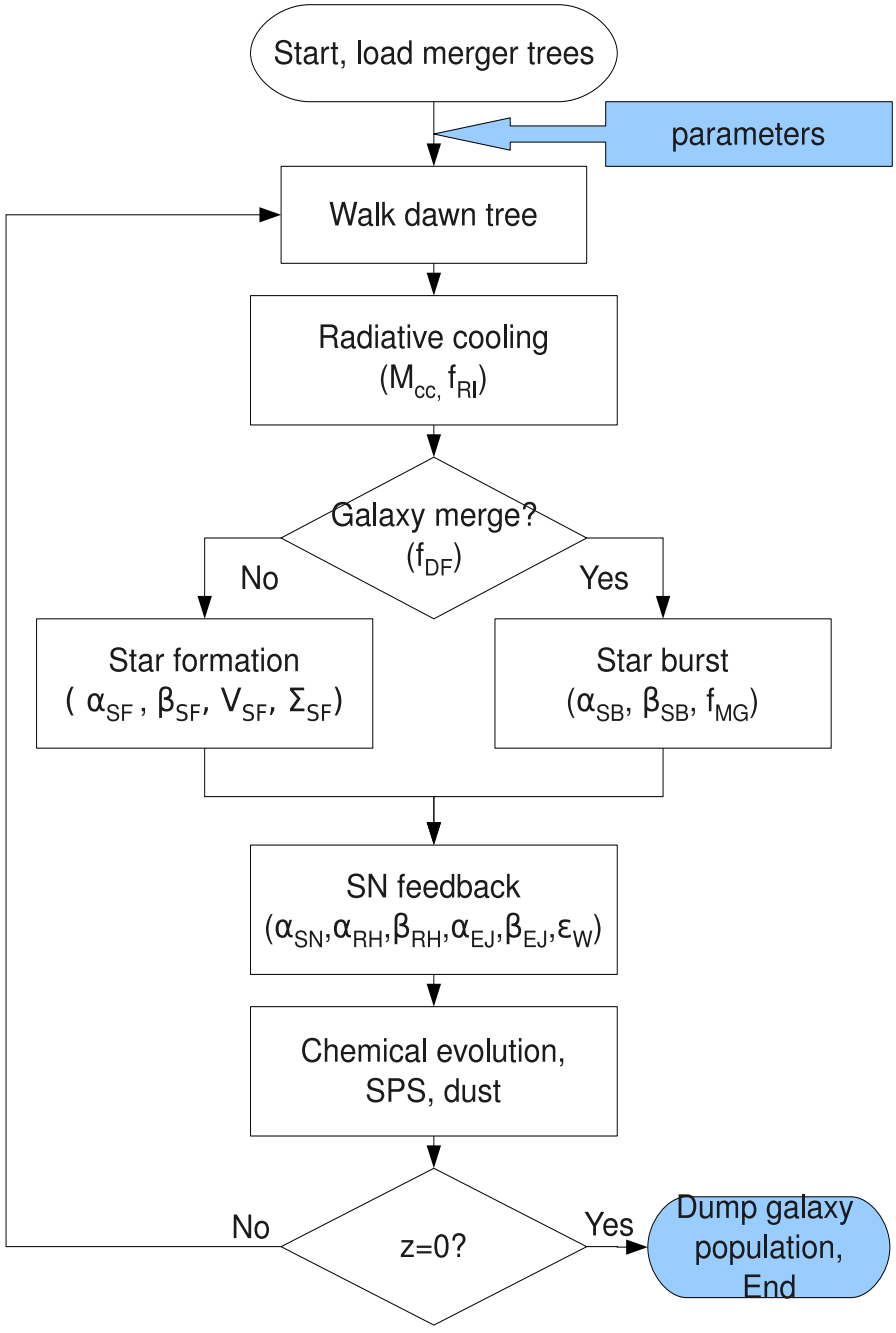

Figure 3: The structure of the SAM. The parameters explored in the these noted in the text.

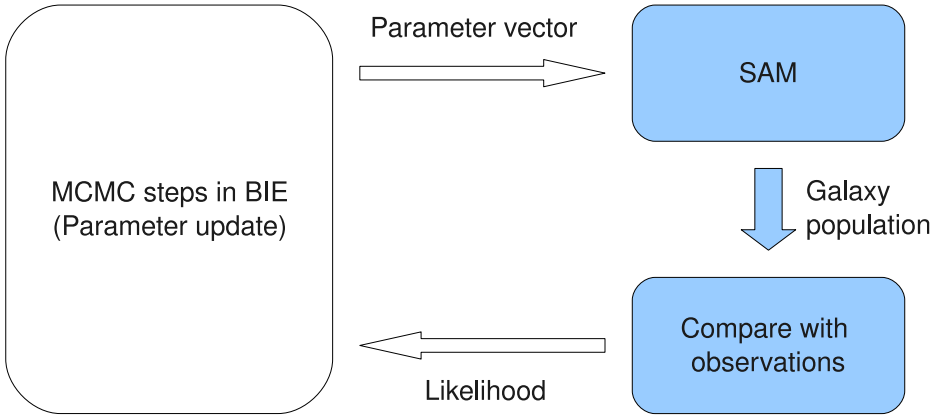

Figure 4: The structure of the Bayesian approach based SAM.

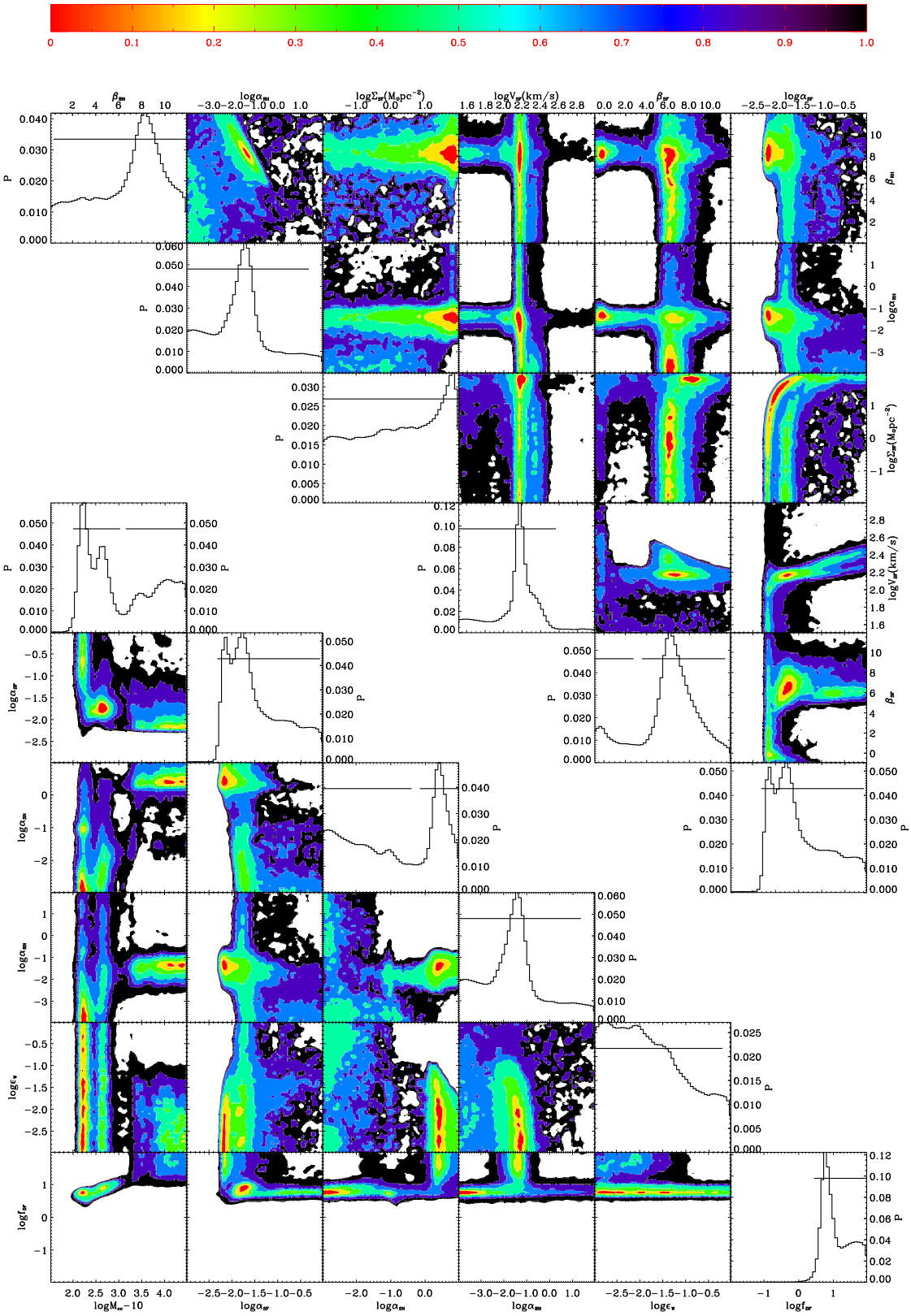

Figure 5: The marginalized posterior distribution of some parameters for Model 0. The color coding represents certain confident level as shown in the upper color-bar. The horizontal bars in the 1-Dimensional marginalized posterior distributions cover the 95% confident range.

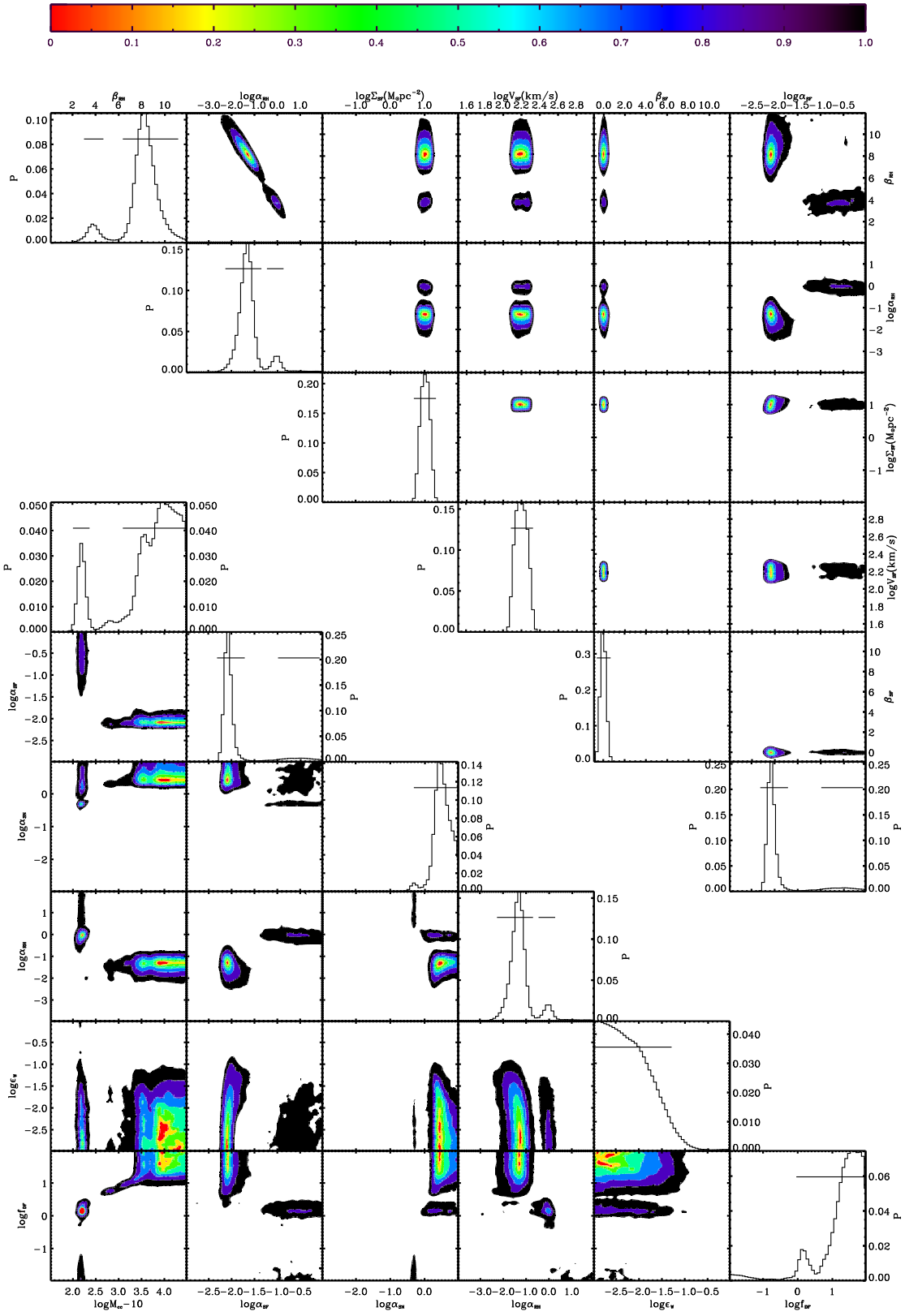

Figure 6: The marginalized posterior distribution of some parameters for Model 1. Note that the parameters, β_{SF}, V_{SF} and Σ_{SF}, in the upper triangle are assigned to have narrow priors.

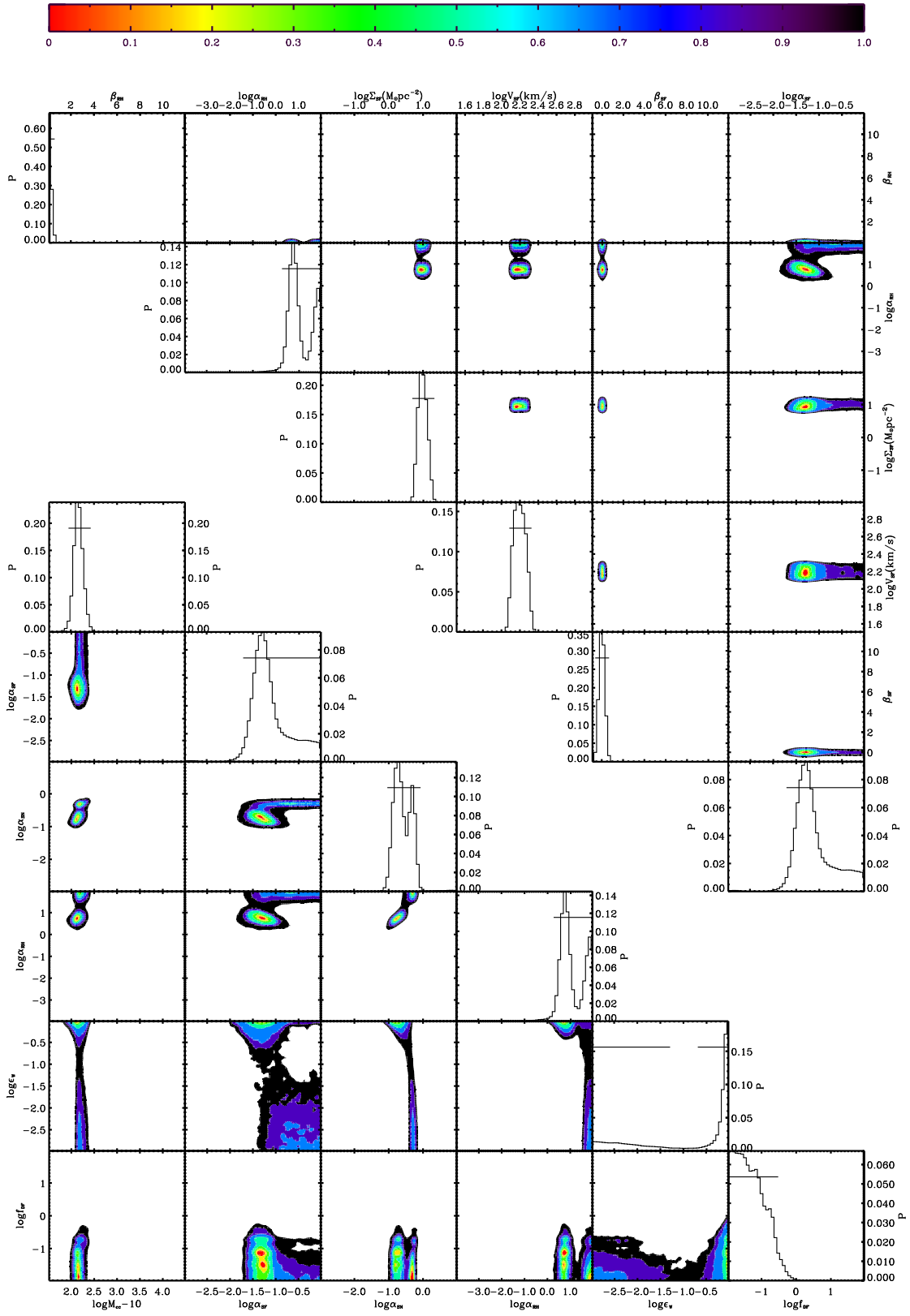

Figure 7: The marginalized posterior distribution of some parameters for Model 2. Note that the parameters, β_{SF}, V_{SF}, Σ_{SF} and β_{RH}, in the upper triangle are assigned to have narrow priors.

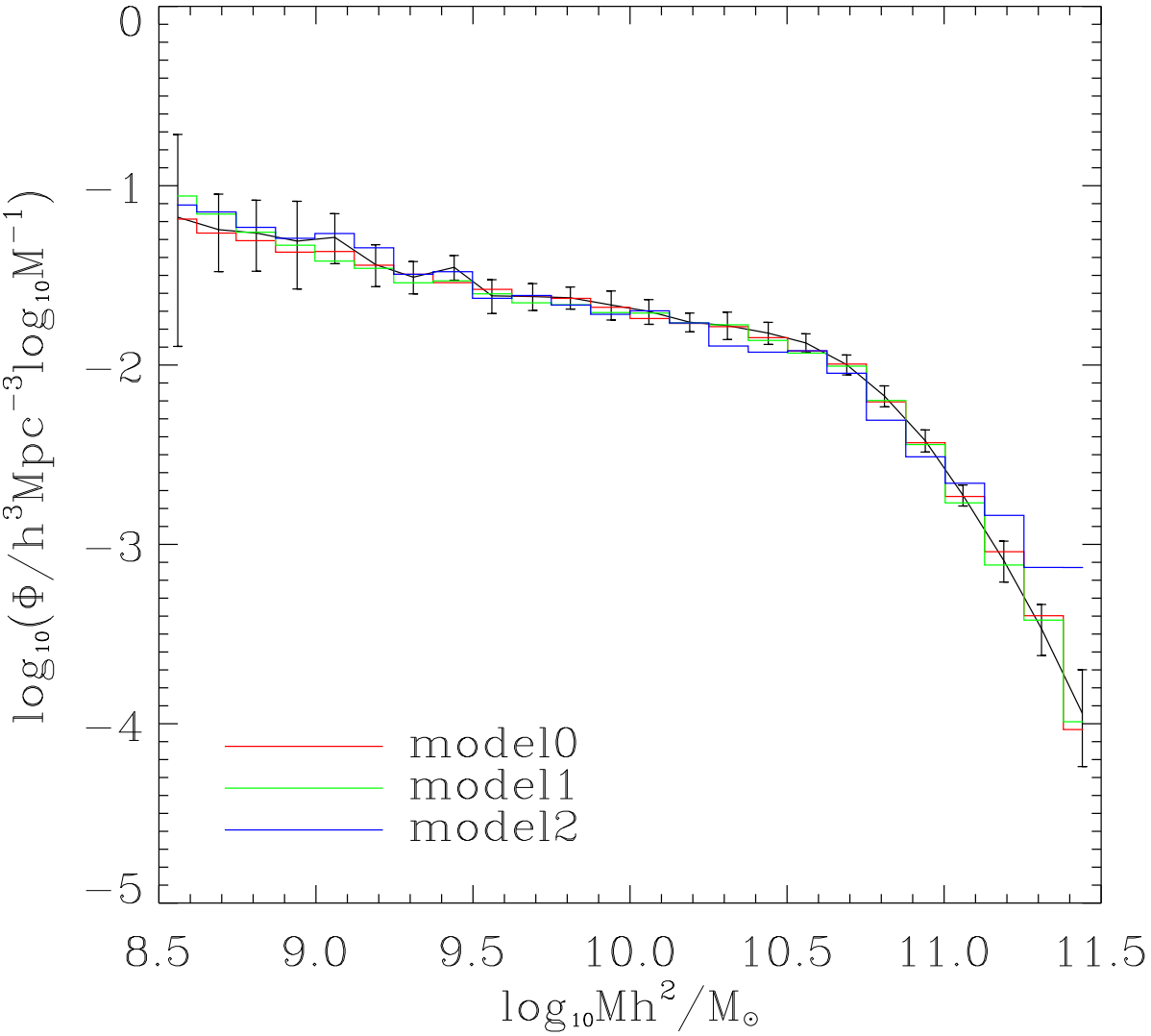

Figure 8: The best fix stellar mass function from the posterior samples of Model 0 (red), Model 1 (green) and Model 2 (blue). The black line with error bars denotes the observations. Note that the plotted error bars are inflated by factor of 3 as used in the likelihood evaluation to accommodate the unknown systematic error in the observation data.